Chain Dynamics in Poly(amido amine) Dendrimers. A Study of ^{13}C NMR Relaxation Parameters

A. Donald Meltzer[†] and David A. Tirrell*

Department of Polymer Science and Engineering, University of Massachusetts, Amherst, Massachusetts 01003

Alan A. Jones* and Paul T. Inglefield

Jeppson Laboratory, Department of Chemistry, Clark University, Worcester, Massachusetts 01610

David M. Hedstrand and Donald A. Tomalia

Michigan Molecular Institute, 1910 W. St. Andrews Road, Midland, Michigan 48640

Received August 5, 1991

ABSTRACT: Two series of poly(amido amine) (PAMAM) dendrimers have been prepared. Both were built from an ammonia core via repetitive addition of methyl acrylate and ethylenediamine. End groups were either hydroxyl or amine, the former derived from 2-aminoethanol substituted for ethylenediamine in the final amidation step. The dynamic properties of these polymers have been examined with the aid of ^{13}C NMR relaxation measurements. Spin–lattice relaxation times (T_1) of the terminal carbons of the hydroxyl-terminated PAMAM in DMSO-d_6 were found to decrease as the number of chain termini increased from 3 (T_1 = 0.54 ± 0.01 s at 75 MHz) to 3072 (T_1 = 0.23 ± 0.01 s at 75 MHz). Decreases in the nuclear Overhauser enhancement (NOE) were also observed; NOE varied from 2.9 ± 0.2 to 2.4 ± 0.2 over this range of molecular size. T_1 was found to increase with temperature, sensitivity to temperature decreasing with increasing molecular weight. The T_1 values of the methylene carbons in the molecular interior were found to decrease initially with molecular weight but were independent of molecular weight above the second generation. The values of T_1 determined at lower field strength (4.70 T) were lower than those at higher field strength (7.05 T), but consistent correlation times (τ) were obtained at both frequencies upon the application of Schaefer's log χ^2 distribution function. The τ calculated for the terminal ^{13}C (2.6×10^{-11} to 6.3×10^{-11} s) varied only weakly with molecular weight. In contrast, τ was found to be a sensitive function of molecular size for the internal ^{13}C, ranging from 7.4×10^{-11} to 1.2×10^{-8} s. Similar results were obtained for hydroxyl-terminated PAMAM dissolved in D_2O and for the amine-terminated dendrimers in either DMSO-d_6 or D_2O. These results indicate that the chain dynamics are insensitive to any steric crowding that may occur at the molecular surface, but report instead a slowing of internal chain motions as molecular size increases.

Introduction

Dendritic macromolecules (dendrimers) represent an intriguing new approach to the control of molecular organization on the colloidal scale. Through the use of iterative branching strategies developed by Tomalia[1–10] and Newkome[11–15] and their co-workers or through the convergent approaches of Hawker and Frechet[16,17] or Miller and Neenan,[18] one can create dendritic structures on size scales comparable to those of surfactant micelles or vesicular aggregates.[19] In contrast to conventional colloids, however, dendrimers are characterized by extensive skeletal interconnections throughout the colloidal volume and thus offer the prospect of partitioning that volume with a level of control unattainable in vesicles or micelles.

The synthesis of dendritic poly(amido amine)s (PAMAM) involves the reaction of a nucleophilic initiator core (e.g., ammonia) with a multifunctional electrophilic reagent (e.g., methyl acrylate) which carries functional groups of significantly different reactivities toward the initiator core (Scheme I). Reaction of the resulting adduct (1) with a large molar excess of a multifunctional nucleophile (e.g., ethylenediamine) produces a compound of increased terminal multiplicity, with terminal nucleophilic sites that can serve to expand the system further upon repetition of the growth cycle. Through such a reaction sequence, a highly symmetrically branched condensation polymer can be prepared. This particular construction leads to dendrimers in which the number of branch points doubles with each successive cycle. To ensure creation of the ideal dendritic topology, all reaction steps must be essentially quantitative. Furthermore, the reactions must be performed under conditions that avoid intermolecular bridging, intramolecular "looping", retro-Michael additions, and other competitive reactions. We[8a] and Smith and co-workers[8b] have examined these flawed structures carefully and established conditions under which the failure rate per growth cycle can be reduced to 1–2%.

Several theoretical treatments have been developed to describe the behavior of dendrimers.[20–25] Specifically, de Gennes[20] has suggested that "ideal starbust growth" is restricted to a limiting size, since the perfect cascade branching process must break down at some limiting value of the segmental packing density. Above this limit, the branching pattern will be interrupted by overcrowding of the end groups. Maciejewski[21] has proposed that large dendritic molecules should be capable of forming an outer barrier, or shell, that restricts access to the interior of the molecule. The formation of such a barrier is of course an extreme case of the dense packing described by de Gennes. Should such a barrier form, the resulting dendrimers might find important applications, perhaps as sequestering agents or in controlled-delivery systems.[3,9]

Molecular dynamics simulations of PAMAM dendrimers have been performed by Naylor and Goddard.[22,23] The simulations indicate that the overall molecular shape changes as the polymer is grown from generation 0 to

[†] Present address: C.E.R.S.I.M., Department of Chemistry, Laval University, Saint Foy, Quebec, Canada G1K 7P4.

0024-9297/92/2225-4541$03.00/0

Scheme I
Synthesis of Poly(amido amine) Dendrimers

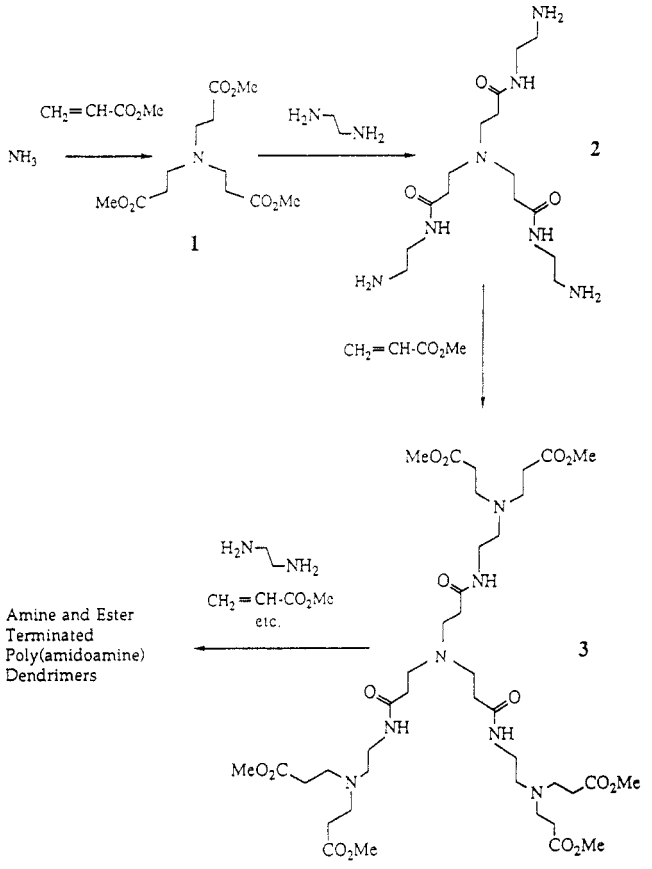

generation 6. Internal cavities and channels appear at generations ≥3, following a transition from open, extended structures at lower generations. The simulations indicate that approximately 50% of the internal volume is a "solvent-filled void", from which it was concluded that the internal regions could be used for sequestering small molecules. Radial density distributions, which would provide greater insight into the chain conformations and potential for enhanced surface densities or barrier properties, were not published.

By simulating the growth of dendritic molecules, Lescanec and Muthukumar[24] have also made predictions about the behavior of molecules of this new topology. Their model suggests that there is an increase in monomer density in the interior of the molecules as molecular weight increases, owing to a folding back of chains into the interior of the dendrimer.

These contradictory predictions demonstrate the need for fundamental experimental investigation of molecules with dendritic topology. The present paper describes an exploration of PAMAM dendrimers via NMR methods. Dynamic NMR has already been applied to the examination of host–guest interactions in these dendrimer systems.[25] Naylor and co-workers have used the technique to demonstrate a strong interaction between PAMAM dendrimer hosts and certain carboxylic acid guests in $CHCl_3$ solution. The spin–lattice relaxation times (T_1) of the aromatic carbon nuclei of the acids were shown to depend on the molecular size of the codissolved dendrimer. We describe herein direct measurements of the ^{13}C NMR relaxation behavior of PAMAM dendrimers dissolved in DMSO-d_6 or in D_2O. The results provide insight into the chain dynamics of dendrimers and are interpreted in terms of the alternative theoretical treatments of such systems.

Experimental Section

Materials. 2-Aminoethanol was distilled over CaH_2 under reduced pressure (bp 59–63 °C/4 Torr). Ethylenediamine (EDA) was distilled over CaH_2. Methyl acrylate (MA) was cryogenically distilled (bp 18–25 °C/4 Torr). All other compounds, unless otherwise specified, were of the highest grade available from Aldrich Chemical Co. and were used as received.

Preparations. Hydroxyl-Terminated PAMAM. Half-generation PAMAM dendrimers (0.2 g, 1 mmol of end groups) prepared as described previously[1] were dissolved in 50 mL of methanol. The solutions were deoxygenated by passing a flow of N_2 through the solution for no less than 30 min. Distilled 2-aminoethanol (10 mL, 170 mmol) was added by syringe. The solutions were stirred at room temperature for 9 days, after which the solvent was removed under reduced pressure. The polymers of fifth and higher generations were purified by dialysis against methanol using Spectropore cellulose membranes with a molecular weight cutoff of 1000. The excess amionethanol was removed from the lower molecular weight polymers by repetitive azeotropic distillations under a reduced pressure of a 4:1 mixture of methanol and toluene. The procedure was repeated until it was not possible to detect the presence of aminoethanol in the distillate by gas chromatography (residual levels were estimated to be <1% by weight). ^1H NMR (200 MHz, D_2O): 3.45, 3.18, 2.67, 2.48, 2.24 ppm. ^{13}C NMR (50 MHz, D_2O): 177.9, 177.4, 63.1, 54.5, 52.2, 44.6, 36.8, 33.8 ppm. IR (neat): 3300, 2940, 2870, 1645, 1560, 1070 cm^{-1}.

Amine-Terminated PAMAM. Generation 0 PAMAM.[26] Into a 250-mL round-bottom flask was placed 120 mL of methanol (MeOH). The solvent was deoxygenated by bubbling a steady stream of N_2 through it for no less than 30 min. Ammonia was then bubbled through the MeOH, and the amount added (5.0 g, 0.29 mol) was determined by measuring the increase in mass of the reaction flask. MA (90 g, 1.05 mol) was cannulated into the reaction flask. The reaction vessel was left stirring at room temperature in the dark for 36 h, at which time all volatile materials were removed under reduced pressure (15–20 Torr) to provide a quantitative yield (80 g) of 1. ^1H NMR (300 MHz, $CDCl_3$): 3.65 (s, 3 H), 2.75 (t, 2 H), 2.43 (t, 3 H) ppm. ^{13}C NMR (50 MHz, $CDCl_3$): 172.0, 51.6, 49.4, 32.8 ppm. IR (neat): 2950, 2850, 1730, 1440, 1370, 1320, 1180, 1040, 850 cm^{-1}.

A 10% solution of 1 (2.0 g, 7.3 mmol) in MeOH was deoxygenated by bubbling a steady stream of N_2 through the solution for no less than 30 min. The solution was cannulated into an excess (50-fold by weight, 76-fold on a molar basis) of distilled EDA (100 g, 1.7 mol) which had been cooled to 0–5 °C in an ice bath. The solution was stirred at 0–5 °C for 4 days, after which time the solvent and EDA were removed under reduced pressure (15–20 Torr). The residual amine was removed by repetitive azeotropic distillations as follows. The sample was dissolved in 10 mL of MeOH, and 120 mL of toluene was added to the mixture. The volatile material was then removed on a Buchi rotary evaporator under reduced pressure (35 °C, 15–20 Torr). Repetition of the procedure twice proved to be sufficient to remove the residual EDA to the point where the amine was undetectable by gas chromatography (residual levels in the dendrimer were estimated to be <1% by weight). The reaction provided a quantitative yield of 4.8 g of generation 0 PAMAM. ^1H NMR (300 MHz, $CDCl_3$): 3.05 (t, 2 H), 2.61 (t, 2 H), 2.52 (t, 2 H), 2.24 (t, 2 H) ppm. ^{13}C NMR (50 MHz, D_2O): 178.0, 50.0, 42.9, 41.0, 33.8 ppm. IR (neat): 3300, 3080, 2950, 2850, 1640, 1550, 1470, 1440, 1360, 1290, 1140, 1040, 930 cm^{-1}.

Generation 0.5 PAMAM. Generation 0 PAMAM (2.0 g, 5.6 mmol or 34 mmol of end groups) was dissolved in 10 mL of MeOH in a 20-dram vial fitted with a rubber septum. The solution was deoxygenated as described above. To the solution was added 4.0 mL (44 mmol) of MA. The reaction mixture was stirred for 36 h at room temperature, and volatile materials were removed under reduced pressure (35 °C, 15–20 Torr) to provide a quantitative yield (2.9 g) of generation 0.5 PAMAM. ^{13}C NMR (50 MHz, $CDCl_3$): 177.4, 171.8, 53.0, 51.6, 49.3, 37.1, 33.6, 33.3, 32.7 ppm. IR (neat): 3300, 2950, 2820, 1740, 1650, 1520, 1440, 1180, 1050, 850 cm^{-1}.

Full-Generation (Amine-Terminated) PAMAM. The procedure followed in the syntheses of these dendrimers is similar

Table I
Excess EDA Used in the Synthesis of PAMAM Dendrimers

generation	EDA:PAMAM[a]	generation	EDA:PAMAM[a]
1	50	6	730
2	60	7	1440
3	100	8	2870
4	200	9	5740
5	370		

[a] By weight.

to that used to prepare generation 0 PAMAM and begins in each case with the appropriate half-generation sample. Larger excesses of EDA were used; the exact weight ratios are listed in Table I. The syntheses of generations 2 and higher required the addition of 10% MeOH to the amine prior to cooling in order to lower the freezing point of the amine below the reaction temperature. For dendrimers of sufficient molecular weight (i.e., above generation 2), the residual amine, trapped in the polymer after attempted removal under reduced pressure, was removed via ultrafiltration (cf. Measurements section). ^{13}C NMR (50 MHz, D_2O): 178.0, 177.4, 52.3, 50.1, 49.6, 42.7, 40.9, 37.8, 33.9, 33.7 ppm. IR (neat): 3300, 3080, 2950, 2850, 1640, 1550, 1470, 1440, 1360, 1290, 1140, 1040, 930 cm^{-1}.

Half-Generation (Ester-Terminated) PAMAM. The procedure used for synthesis of generation 0.5 PAMAM was followed starting with the appropriate full-generation PAMAM.

Measurements. ^1H NMR spectra were obtained using Varian XL-200, XL-300, and CFT-20 nuclear magnetic resonance spectrometers at frequencies of 200, 300, and 80 MHz, respectively. ^{13}C NMR spectra were obtained on Varian XL-200 and XL-300 spectrometers operating at 50 and 75 MHz, respectively. ^2H NMR spectra were obtained on a Varian XL-300 spectrometer operating at 46.0 MHz. Chemical shifts (δ) are reported in parts per million (ppm) downfield from tetramethylsilane (TMS). For samples that did not contain TMS, the chemical shifts were referenced to the published shifts of resonances from the lock solvent. All of the spin–lattice relaxation time (T_1) measurements were performed using the standard inversion–recovery method with a pulse sequence 180°–variable delay–90°–acquisition–fixed delay. The temperature inside the probe was maintained at 25 ± 0.2 °C by passing a steady flow of air over the sample. The concentration of polymer was approximately 3% in all cases. Choices of delay times and actual T_1 calculations were performed using standard commands (DOT1 and T1(all)) contained within the standard Varian VXR version 4.1 software package.

Infrared spectra were obtained on Perkin-Elmer 283 and 1320 infrared spectrometers. All spectra were referenced to the 1601-cm^{-1} band of a thin polystyrene film.

Gel permeation chromatographic measurements were made on a Waters instrument, using dimethylformamide as the carrier solvent, a flow rate of 1.0 mL/min, and three μ-Bondagel columns (E-1000, E-500, and E-125) in series. Peak molecular weights were estimated on the basis of a calibration curve derived from four narrowly dispersed poly(ethylene oxide) standards obtained from Scientific Polymer Products, Inc.

Polymers were purified by ultrafiltration employing an S1Y3 spiral-wound membrane cartridge from Amicon (molecular weight cutoff 3000; 1 sq ft of membrane area). The aqueous polymer solutions were pumped through the cartridge by a Masterflex peristaltic pump at a rate of approximately 1 L/h while maintaining a pressure of 20–25 psi over the membrane.

Residual ethylenediamine and 2-aminoethanol contents of the polymers were analyzed by gas chromatography, performed on a Varian 1400 gas chromatograph (6-ft glass column; 10% sp-100 on 80/100 mesh Supelcoport; column 150 °C for ethylenediamine, 178 °C for 2-aminoethanol; injector 200 °C, detector 190 °C; flame ionization detection).

Results and Discussion

Two series of dendrimers of the PAMAM type introduced by Tomalia and co-workers[1-9] but differing in the nature of the end groups (hydroxyl or amine) have been prepared for a study of segmental mobility. Preparing polymers with hydroxyl end groups not only removes problems associated with oxidation of the primary amine termini and cross-linking of the PAMAM that can occur by transamidation but also facilitates the determination of the influence of the end group on chain dynamics. Segmental mobility was studied by ^{13}C NMR relaxation measurements.

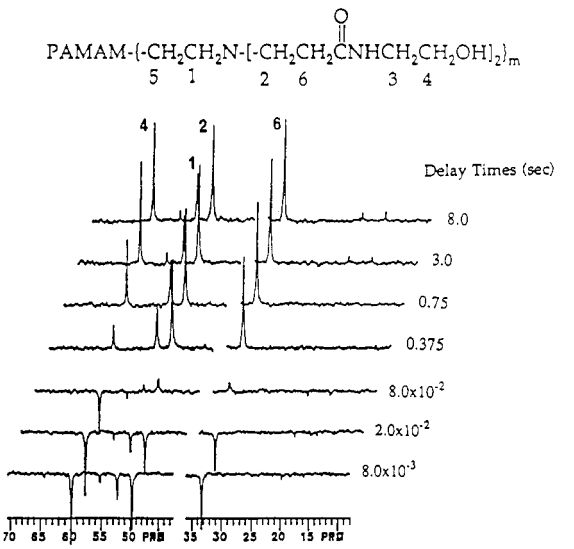

Figure 1. An inversion–recovery experiment from which the T_1 of a generation 4 PAMAM with hydroxyl end groups was calculated (75 MHz, DMSO-d_6, 30 °C).

Hydroxyl-Terminated Dendrimers. Relaxation measurements were obtained for a series of 11 hydroxyl-terminated samples of molecular weight varying from 362 to 614 000, i.e., dendrimers of generations 0–10. Relaxation parameters were measured both in D_2O and in DMSO-d_6. In DMSO-d_6, relaxation data were acquired only for the aliphatic carbons that were not obscured by the solvent signals. The solvent obscured the resonances of carbons assigned numbers 3 and 5 in Figure 1; these resonances appear at 43.3 and 38.8 ppm, respectively, in D_2O. The choice of DMSO-d_6 as solvent permitted the observation of the terminal group (at 61.0 ppm) and three internal sites, i.e., carbons 1, 2, and 6 in Figure 1 (at 52.3, 49.9, and 33.8 ppm, respectively). As will be demonstrated below, the observed trends were identical in the two solvents. The relaxation parameters for the carbonyl carbons were not acquired as (i) the relaxation times are typically very long (>2 s), causing the data acquisition to be prohibitively long, and (ii) the relaxation mechanism for carbonyls is, in general, much more complicated than that for protonated carbons.[27-30]

A typical inversion–recovery experiment from which T_1 was calculated is illustrated in Figure 1, and T_1 for each of the observed carbons is plotted as a function of molecular size in Figure 2. The relaxation rates for all of the interior carbons in a given dendrimer are indistinguishable and are independent of size for dendrimers grown through two or more full generations. Chemically similar carbons in the interior generations have identical chemical shifts, and as a result the T_1 values reported for interior carbons are averages over all interior generations.[31] The relaxation of the interior carbons is faster than that of the carbon nuclei at the chain termini, and the relaxation rate of the terminal hydroxylated carbon decreases with increasing molecular weight over the entire range studied.

The nuclear Overhauser enhancement (NOE) of each signal was determined by comparison of relative peak heights from spectra obtained using continuous broad-band ^1H decoupling and gated decoupling, i.e., with the decoupler only on during the acquisition period. The

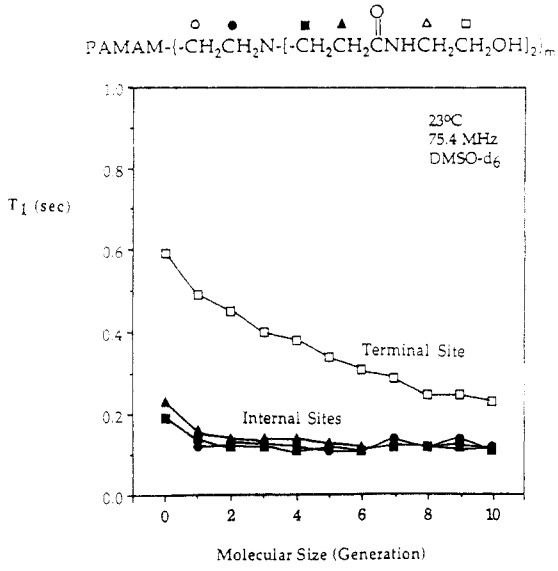

Figure 2. Dependence of T_1 on molecular size for hydroxyl-terminated PAMAM (75 MHz, DMSO-d_6, 23 °C).

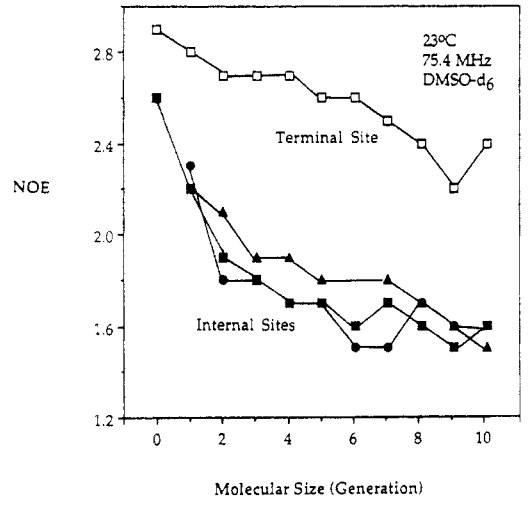

Figure 3. Dependence of NOE on molecular size for hydroxyl-terminated PAMAM (75 MHz, DMSO-d_6, 23 °C). Symbols as in Figure 2.

observed NOE's are plotted in Figure 3. The NOE of 2.9 ± 0.2 for the terminal carbon of the smallest dendrimer is within experimental error of the maximum value of 2.988 associated with relaxation that occurs entirely by the dipole–dipole (DD) mechanism in rapidly reorienting systems[29] and indicates that conversion of the relaxation data to correlation times (τ) based entirely on DD relaxation is applicable.[27] The NOE's of the interior carbons were determined to be slightly smaller. The small values can be associated with slow rotational motions,[27-30] and such an explanation is consistent with the small T_1 values. The NOE becomes independent of molecular weight, but, unlike T_1 of the interior carbons, the NOE is still dependent on molecular weight up to generation 6. This apparent contradiction suggests that the correlation times are in the vicinity of the T_1 minimum, and hence the effects of the topology on chain dynamics are best discussed in terms of τ.

Both T_1 and NOE were determined as a function of temperature (Figures 4 and 5). In all cases T_1 of the terminal carbon increased with temperature, suggesting that $\omega\tau < 1$. The sensitivity of T_1 to temperature was observed to decrease with increasing molecular weight. The T_1 values determined for the interior carbons were less temperature dependent than those of the terminal

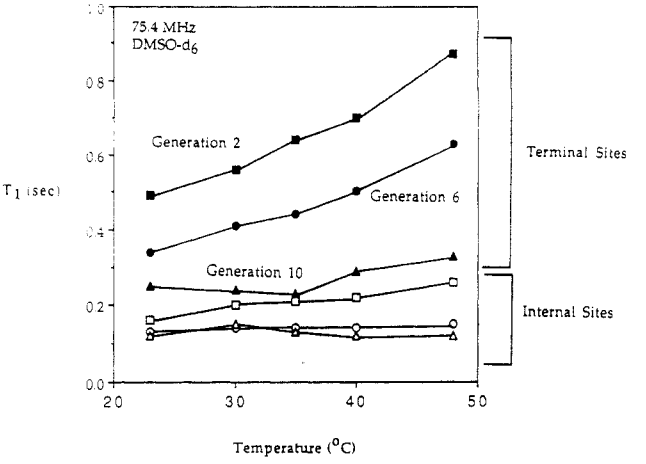

Figure 4. Dependence of T_1 on temperature for hydroxyl-terminated PAMAM for (i) internal sites (generation 2, □; generation 6, ○; generation 10, △) and (ii) terminal sites (generation 2, ■; generation 6, ●; generation 10, ▲) (75 MHz, DMSO-d_6).

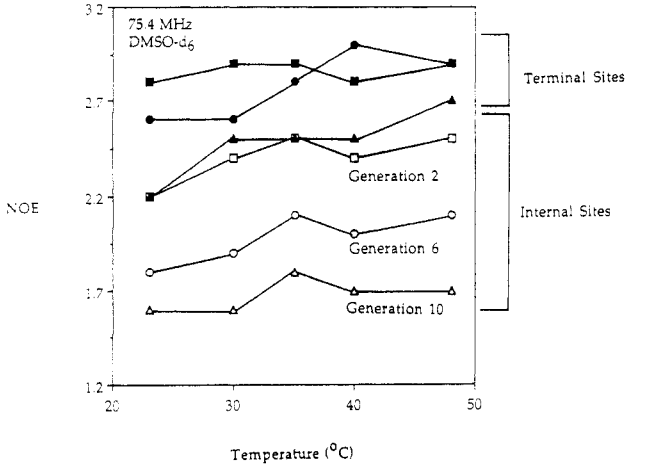

Figure 5. Dependence of NOE on temperature for hydroxyl-terminated PAMAM. Symbols as in Figure 4.

sites, and, in this case as well, the temperature dependence decreased with increasing molecular weight. This, along with the observed weak dependence of NOE on temperature (Figure 5), suggest that some cooperative motion, and therefore a broad distribution of τ, exists. It also suggests that the molecular motions responsible for the relaxation of the interior ^{13}C are such that these measurements have been made in the vicinity of the minimum of the T_1–τ curve. As such, small changes in T_1 would be indicative of relatively large changes in τ. The relaxation times of the terminal carbons, being larger than those observed for the interior sites, would then be further away from the minimum, and T_1 would be more sensitive to changes in τ.

The analysis of the experimental T_1 data to obtain a characterization of the time scale of the motion requires a determination of the relaxation mechanism and a description in terms of a correlation time. The theoretical maximum NOE observed for the terminal carbon of generation 0 at 25 °C suggests domination by the dipole–dipole mechanism. A comparison of T_1 for the deuterated and protonated carbon β to the carbonyl for generation 0 (T_{1,CH_2} = 0.32 ± 0.03 s; T_{1,CD_2} = 3.7 ± 0.4 s) limits the non-dipole–dipole relaxation to about 2.5%.[23] An overall description in terms of a dipole–dipole mechanism thus appears appropriate.

The experimental T_1's also show a frequency dependence, T_1 at 50 MHz being lower than T_1 at 75 MHz in

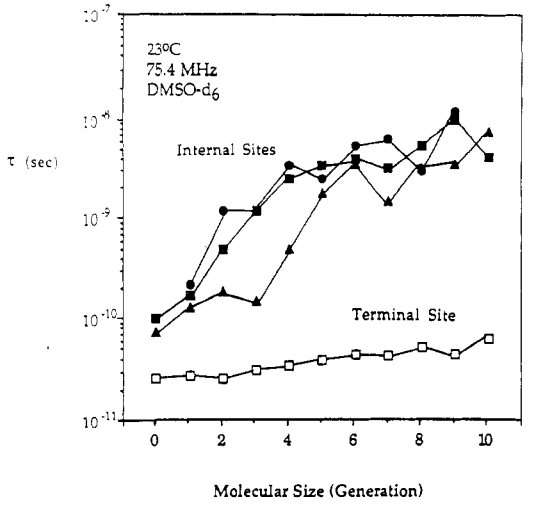

Figure 6. Dependence of τ on molecular size for hydroxyl-terminated PAMAM (75 MHz, DMSO-d_6, 23 °C). Symbols as in Figure 2.

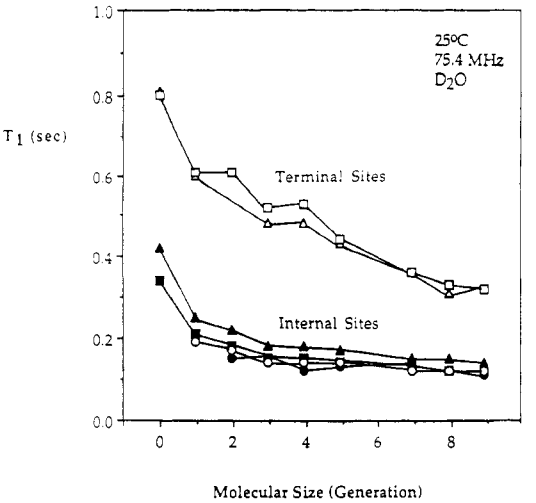

Figure 7. Dependence of T_1 on molecular size for hydroxyl-terminated PAMAM (75 MHz, D_2O, 25 °C). Symbols as in Figure 2.

general; and the T_1's for the interior carbons show very little temperature dependence over the range studied. These observations indicate that a distribution of correlation times may well be necessary to simulate the data. An appropriate, though not unique, choice of distribution is the log χ^2 distribution developed by Schaefer;[33] the formulation is as follows. Schaefer showed that

$$1/T_1 = 0.4(\pi h\gamma_H\gamma_C)^2 r^{-6} N\{J(\omega_C - \omega_H) + 3J(\omega_C) + 6J(\omega_C + \omega_H)\} \quad (1)$$

and

$$\mathrm{NOE} = 1 + \frac{-J(\omega_C - \omega_H) + 6J(\omega_H)}{J(\omega_C) + 4J(\omega_C + \omega_H)} \quad (2)$$

where

$$J(\omega) = \int \frac{F(s)\{b^2 - 1\}\,ds}{(b-1)(1 + \omega^2\tau^2[(b^s - 1)/(b-1)]^2)} \quad (3)$$

where

$$s = \log_b [1 + (b-1)\tau_0/\tau] \quad (4)$$

and

$$F(s) = P\Gamma(P)^{-1}(P^s)^{P-1} \exp(-Ps) \quad (5)$$

Here, $\Gamma(P)$ represents the gamma function, b, P, and τ (and τ_0, which is defined to be proportional to τ) are chosen to fit the data, ω_C and ω_H represent the resonance frequencies of ^1H and ^{13}C, respectively, h is Planck's constant, r is the C–H internuclear distance, N is the number of covalently bonded ^1H, and γ_C and γ_H are the gyromagnetic ratios of ^{13}C and ^1H, respectively. It is generally agreed that b and P, which control the width of the distribution of τ, are not totally independent and that the model is essentially a pseudo-two-parameter model.[27] Values of τ were calculated by assuming $b = 1000$ in eq 3 and fitting P and τ to the measured T_1 and NOE values measured at 75 MHz, making certain that the calculated values of τ and P yielded values of T_1 and NOE that fell well within the experimental error of those measured at 50 MHz.

The dependence of τ on molecular weight is illustrated in Figure 6. For the terminal carbon, τ exhibits a linear dependence on generation, with a small positive slope. This is somewhat surprising as any dependence on molecular weight is atypical of linear high polymers. It has been demonstrated, both by fluorescence depolarization experiments[34] and by electron spin resonance,[35] that the mobility of the end group is dominated by local segmental motions for polymers of molecular weight >30 000 and, as such, is independent of molecular size. On the other hand, there is nothing in these results to suggest that increasing segment density near the "surface" of the dendritic structure leads to any anomalous suppression of chain dynamics, even for molecules grown through as many as 10 generations. Indeed, the mobility of the end groups appears always to be greater than that of the interior carbons.

Perhaps the most striking result shown in Figure 6 is the marked molecular weight dependence of τ for the interior carbon sites. Typically, the segmental mobility of polymer chains becomes independent of molecular weight once a certain critical degree of polymerization is reached.[36-42] The sensitivity of τ to the size of the dendritic PAMAM structure, even for molecular weights of several hundred thousand, most likely results from an increase in segment density in the molecular interior. These observations appear to be consistent with the theoretical treatment of Lescanec and Muthukumar,[24] which predicts that the segment density in the vicinity of the end groups is below the level where concentration effects have been observed for linear polymers,[38] i.e., below 10% volume fraction, thus explaining the small molecular weight dependence observed for τ of the terminal carbons. In contrast, the calculated[24] segment density inside the dendritic structure is significantly higher than that in the vicinity of the end groups and is in the region where NMR relaxation data for linear polymers depend on concentration.[38] Furthermore, the interior segment density is predicted to increase with molecular size and thus may account for the observed dependence of τ on molecular weight for the interior carbons.

Relaxation in D_2O. The relaxation behavior of the hydroxyl-terminated dendritic PAMAM in D_2O was in all respects similar to the behavior observed in DMSO-d_6. Figures 7 and 8 show the variation in T_1 and τ, respectively, with molecular weight for these samples. As described above, T_1 is largest for the terminal carbon sites and decreases for those sites over the full range of molecular weights. For the interior carbons, T_1 is smaller and virtually independent of molecular size at generations 2 and above. The calculated correlation times increase modestly with molecular size for the terminal carbons and

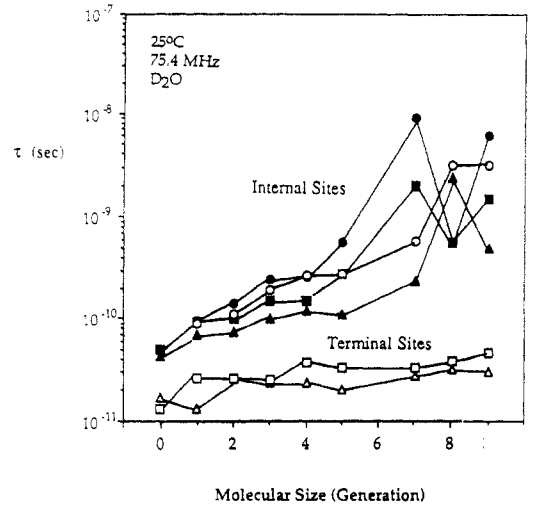

Figure 8. Dependence of τ on molecular size for hydroxyl-terminated PAMAM (75 MHz, D_2O, 25 °C). Symbols as in Figure 2.

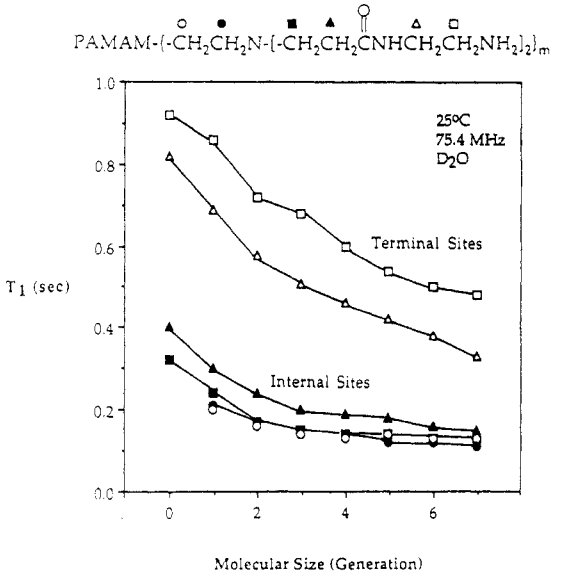

Figure 9. Dependence of T_1 on molecular size for amine-terminated PAMAM (75 MHz, D_2O, 25 °C).

more rapidly for the interior sites. Thus the results reported herein do not appear to be affected in an important way by specific interactions between polymer and solvent.

Amine-Terminated Polymers. Relaxation parameters were determined for the amine-terminated series of dendritic PAMAM polymers in DMSO-d_6, in D_2O, and in mixtures of DMSO-d_6 and H_2O. The range of molecular sizes examined was restricted to generations 0–7 (molecular weights 360 to 87 300). The results in the three solvent systems were fully consistent, with the exception of the fact that somewhat larger values of τ were observed in DMSO-d_6 as compared to D_2O. Because D_2O allows observation of all of the resonances of the sample while DMSO-d_6 obscures those due to the terminal carbons, we present in Figures 9–11 only the results obtained in D_2O.

These data illustrate again the trends described above: (i) T_1 for the terminal carbons is large and decreases over the full range of molecular sizes, (ii) T_1 for the internal sites is small and virtually invariant above generation 2, (iii) the NOE is near-maximal for the terminal carbons and declines with molecular size, particularly in the interior of the dendritic structure, and (iv) τ increases modestly with molecular size at the chain termini and more steeply

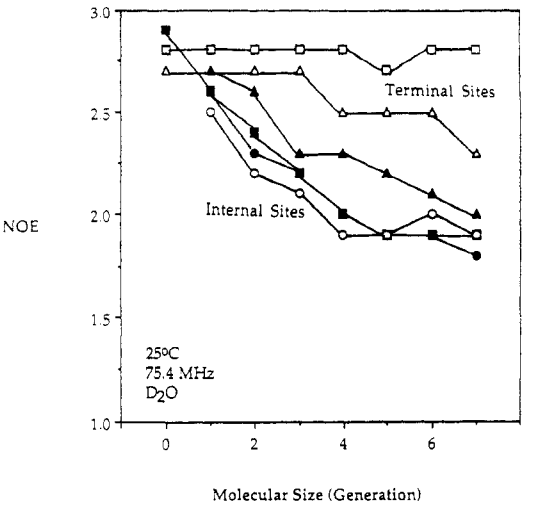

Figure 10. Dependence of NOE on molecular size for amine-terminated PAMAM (75 MHz, D_2O, 25 °C). Symbols as in Figure 9.

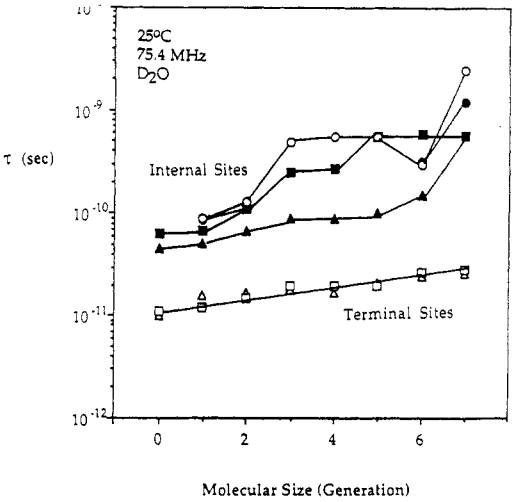

Figure 11. Dependence of τ on molecular size for amine-terminated PAMAM (75 MHz, D_2O, 25 °C). Symbols as in Figure 9.

for the interior carbons. These trends thus appear to be quite general for these dendritic macromolecules, in that they recur for samples of differing end group functionality and variable solvent composition.

Concluding Remarks. The iterative branching process that creates the dendritic PAMAM architecture must at some point lead to severe steric crowding either at the molecular surface or throughout the volume of the molecule. The maximum possible surface area increases as G^2 and the number of terminal groups increases as 2^G. If the terminal groups do not reside on the molecular surface, total density becomes a second criterion, with maximum molecular volume increasing as G^3 and molecular weight increasing as $2^{G+1} - 1$. In either case, the exponential term grows at a rate that must overwhelm the square or cubic term, giving a limiting generation. Arrival at this congested state is proposed to be manifested with some change in physical properties.[9] A primary motivation of the work described herein was to determine whether or not the approach to the congested state would be signaled by an anomalous suppression of local chain dynamics. No sudden change in dynamics that could be considered anomalous was observed. Throughout the range of molecular sizes examined (G = 0–10), there was a gradual slowing of molecular motions, which suggests a gradual

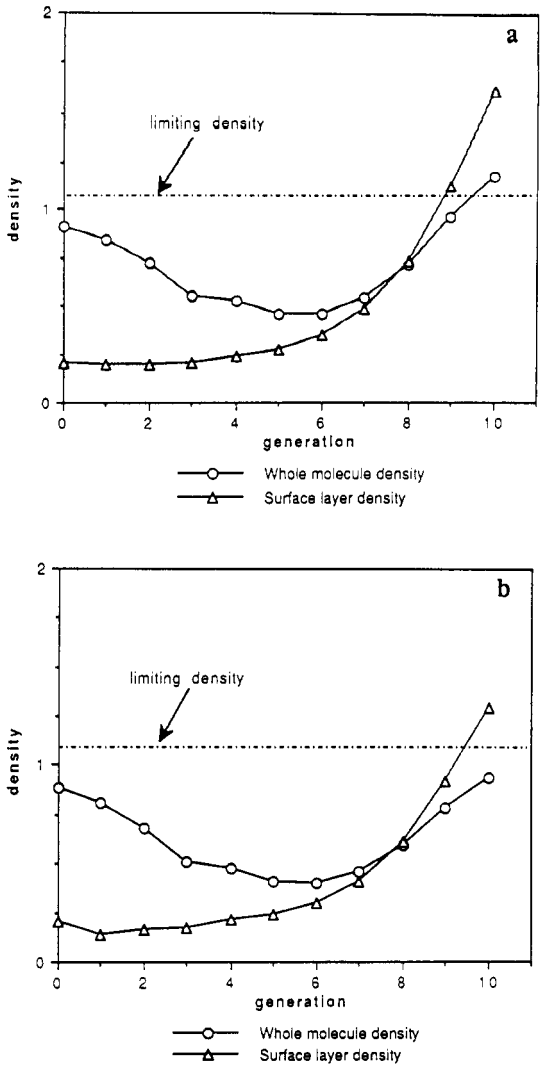

Figure 12. Calculated molecular (O) and surface layer (Δ) densities for PAMAM dendrimers prepared (a) under conditions of ideal (defect-free) branching and (b) with a failure rate per generation of 2%.

increase in segment density. These changes did not suggest an exponential approach to a limiting state.

The modest effects on the chain termini suggest that the terminal groups are not densely packed at the surface of the generation 10 dendrimer examined in this work. Ideal branching according to Scheme I would dictate that such a molecule would bear 3072 terminal functional groups. Examination of CPK models[3,9] suggests a maximum molecular radius of ca. 71 Å for this species, and SEC of the amine analog suggests an actual radius of ca. 62 Å. An ideal dendrimer in a fully extended conformation would have an area of ca. 21 Å^2 per terminal group, which is a very dense surface. At the measured hydrodynamic dimensions, there is 16 Å^2 available per terminal group. Even allowing for a 2% failure frequency per growth cycle increases the available area to only 26 or 19 Å^2 per terminal group, respectively.

These limits are illustrated graphically in Figure 12, which shows the changes in density with generation of the complete dendrimer and the surface layer (assuming all terminal groups are distributed symmetrically on the dendrimer surface) using measured hydrodynamic dimensions. If a reasonable limiting density is chosen (cf. 1.1 for amorphous nylon), it can be seen that the surface of an ideal PAMAM dendrimer of generation 9–10 would be extraordinarily dense. Assuming the 2% growth failure frequency, generation 10 would still have an extraordinarily dense surface.

The mobility of the terminal groups suggests more available area. Therefore, either the number of terminal groups must be much less than that attributable to the 2% growth failure rate, or the conformation must be such that all of the terminal groups do not reside at the surface. This would be consistent with a folding back of terminal groups into the interior of the molecule as suggested by Lescanec and Muthukumar[24] and the dynamic modeling by Naylor and Goddard.[9,22,23] Such conformations would be subject to volume, rather than surface area, limitations. The whole-molecule densities shown in the graphs suggest that no unreasonable densities are implied by the synthesis of a generation 10 PAMAM dendrimer at a 2% growth failure rate. Thus it appears likely that even under the carefully controlled conditions used to prepare the samples used in this work, the dense-packed state is deferred beyond the tenth generation of growth. Within this regime, i.e., prior to the onset of dense packing, the simulation of dendritic growth reported by Lescanec and Muthukumar[24] appears to provide a plausible rationale for the observed relaxation behavior.

Acknowledgment. We express our appreciation to Dow Chemical Co. for funding this work and to Drs. Larry Wilson and Pat Smith, with whom we have had many helpful discussions. NMR spectra were recorded in the University of Massachusetts NMR Laboratory, which is supported in part by the NSF Materials Research Laboratory at the University.

References and Notes

(1) Tomalia, D. A.; Baker, H.; Dewald, J.; Hall, M.; Kallos, G.; Martin, S.; Roeck, J.; Ryder, J.; Smith, P. *Polym. J. (Tokyo)* **1985**, *17*, 117.
(2) Tomalia, D. A.; Baker, H.; Dewald, J.; Hall, M.; Kallos, G.; Martin, S.; Roeck, J.; Ryder, J.; Smith, P. *Macromolecules* **1986**, *19*, 2466.
(3) Tomalia, D. A.; Hedstrand, D. M.; Wilson, L. R. *Encyclopedia of Polymer Science and Engineering*, 2nd ed.; John Wiley and Sons, Inc.: New York, 1990; Index Volume, p 46.
(4) Tomalia, D. A.; Hall, M.; Hedstrand, D. M. *J. Am. Chem. Soc.* **1987**, *109*, 1601.
(5) Tomalia, D. A.; Berry, V.; Hall, M.; Hedstrand, D. M. *Macromolecules* **1987**, *20*, 1164.
(6) Tomalia, D. A.; Dewald, J. R. US Pat. 4507466, 1985; US Pat. 4558120, 1985; US Pat. 4568737, 1986; US Pat. 4587329, 1986; US Pat. 4631337, 1986; US Pat. 4694064, 1987; US Pat. 4713975, 1987; US Pat. 4737550, 1988; US Pat. 4871779, 1989; US Pat. 4857599, 1989.
(7) Tomalia, D. A.; McConnell, J. R.; Padias, A. B.; Hall, H. K., Jr. *J. Org. Chem.* **1987**, *52*, 5305.
(8) (a) Meltzer, A. D. Ph.D. Dissertation, University of Massachusetts, 1990. (b) Smith, P. B.; Martin, S. J.; Hall, M. J.; Tomalia, D. A. *Applied Polymer Analysis and Characterization* Mitchell, J. Jr., Ed.; Hanser Publishers: New York, 1987; p 357.
(9) Tomalia, D. A.; Naylor, A. M.; Goddard, W. A., III *Angew. Chem., Int. Ed. Engl.* **1990**, *29*, 138.
(10) Moreno-Bondi, M. C.; Orellana, G.; Turro, N. J.; Tomalia, D. A. *Macromolecules* **1990**, *23*, 910.
(11) Newkome, G. R.; Yao, Z.; Baker, G. R.; Gupta, V. K. *J. Org. Chem.* **1985**, *50*, 2003.
(12) Newkome, G. R.; Baker, G. R.; Saunders, M. J.; Russo, P. S.; Gupta, V. K.; Yao, Z.; Miller, J. E.; Bouillon, K. *J. Chem. Soc.* **1986**, 752.
(13) Newkome, G. R.; Yao, Z.; Baker, G. R.; Gupta, V. K.; Russo, P. S.; Saunders, M. J. *J. Am. Chem. Soc.* **1986**, *108*, 849.
(14) Newkome, G. R.; Baker, G. R.; Arai, S.; Saunders, M. J.; Russo, P. S.; Theriot, K. J.; Moorefield, C. N.; Rogers, L. E.; Miller, J. E.; Lieux, T. R.; Murray, M. E.; Phillips, B.; Pascal, L. *J. Am. Chem. Soc.* **1990**, *112*, 8458.
(15) Newkome, G. R.; Lin, X. *Macromolecules* **1991**, *24*, 1443.
(16) Hawker, C. J.; Frechet, J. M. J. *J. Am. Chem. Soc.* **1990**, *112*, 7638.
(17) Hawker, C. J.; Frechet, J. M. J. *J. Chem. Soc., Chem. Commun.* **1990**, 1010.
(18) Miller, T. M.; Neenan, T. X. *Chem. Mater.* **1990**, *2*, 346.

(19) Additional synthetic work on hyperbranched or dendritic macromolecules has been reported: (a) Uhrich, K. E.; Boegeman, S.; Frechet, J. M. J.; Turner, S. R. *Polymer Bull.* **1991**, *25*, 551; (b) Mathias, L. J.; Carothers, T. W. *J. Am. Chem. Soc.* **1991**, *113*, 4043; (c) Morikawa, A.; Kakimoto, M.; Imai, Y. *Macromolecules* **1991**, *24*, 3469; (d) Uchida, H.; Kabe, Y.; Yoshino, K.; Kawamata, A.; Tsumuraya, T.; Masamune, S. *J. Am. Chem. Soc.* **1990**, *112*, 7077; (e) Kim, Y. H.; Webster, O. W. *J. Am. Chem. Soc.* **1990**, *112*, 4592.
(20) de Gennes, P.-G.; Hervet, H. *J. Phys., Lett.* **1983**, *44*, 351.
(21) Maciejewski, M. *J. Macromol. Sci., Chem.* **1982**, *A17*, 689.
(22) Naylor, A. M.; Goddard, W. A., III. *Polym. Prepr. (Am. Chem. Soc., Div. Polym. Chem.)* **1988**, *29*, 215.
(23) Naylor, A. M. Ph.D. Dissertation, California Institute of Technology, 1989.
(24) Lescanec, R.; Muthukumar, M. *Macromolecules* **1990**, *23*, 2280.
(25) Naylor, A.; Goddard, W. A., III; Keifer, G. E.; Tomalia, D. A. *J. Am. Chem. Soc.* **1989**, *111*, 2339.
(26) The convention for numbering of generations adopted herein is that proposed by Tomalia and co-workers.[9] In comparison with the numbering scheme proposed earlier (cf. ref 1, for example), this convention reduces by 1 the number of generations assigned to a given PAMAM structure. We retain the convention of referring to the amine-terminated species as "full-generation" PAMAM and to the ester-terminated species as "half-generation" PAMAM.
(27) Levy, G. C. *Topics in Carbon-13 NMR Spectroscopy*; John Wiley and Sons Inc.: New York, 1974; Vol. 1.
(28) Farrar, T. C.; Becker, E. D. *Pulse and Fourier Transform NMR: Introduction to Theory and Methods*; Academic Press: New York, 1971.
(29) Kuhlmann, K. F.; Grant, D. M.; Harris, R. K. *J. Chem. Phys.* **1970**, *52*, 3439.
(30) Schaefer, J.; Natusch, F. S. *Macromolecules* **1972**, *5*, 416.
(31) The numbering and symbolic identification of the carbon atoms in the dendritic structures shown in Figures 1, 2, and 9 are not rigorously correct. Carbons labeled 1, 2, 5, and 6 (Figure 1) are not confined to the terminal and penultimate generations of the structure but represent classes of chemically similar sites located throughout the polymer. We have been unable to devise a concise representation that avoids this ambiguity.
(32) Equations i and ii (for protonated and deuterated carbons, respectively) were applied to a generation 0 amine-terminated PAMAM. Solving the equations for $T_{1,other}$ (given the observed

$$1/T_1 = (h\gamma_H\gamma_C)^2 r^{-6} N + 1/T_{1,other} \quad \text{(i)}$$

$$1/T_1 = {}^8/_3(h\gamma_C\gamma_D)^2 r^{-6} N + 1/T_{1,other} \quad \text{(ii)}$$

values of $T_{1,CH_2} = 0.32 \pm 0.03$ s and $T_{1,CD_2} = 3.7 \pm 0.4$ s) shows that there is a relative contribution of 2.5% to the overall relaxation process from mechanisms other than intramolecular DD of directly bonded ^1H for the ^{13}C β to the carbonyl (Abragam, A. *Principles of Nuclear Magnetism*; Oxford University Press: London, 1961).
(33) Schaefer, J. *Macromolecules* **1973**, *6*, 882.
(34) North, A. M.; Soutar, I. *J. Chem. Soc., Faraday Trans. 1* **1972**, *68*, 1101.
(35) Bullock, A. T.; Cameron, G. G.; Krajewski, V. *J. Phys. Chem.* **1976**, *80*, 1792.
(36) Matsuo, K.; Kuhlmann, K. H.; Yang, W. H.; Geny, F.; Stockmayer, W. H.; Jones, A. A. *J. Polym. Sci., Polym. Phys. Ed.* **1977**, *15*, 1347.
(37) Inoue, Y.; Nishioka, A.; Chujo, R. *J. Polym. Sci., Polym. Phys. Ed.* **1973**, *11*, 2237.
(38) Heatley, F. *Polymer* **1973**, *16*, 493.
(39) Slichter, W. P.; Davis, D. D. *Macromolecules* **1968**, *1*, 47.
(40) Ghesquiere, D.; Ban, B.; Chochaty, C. *Macromolecules* **1977**, *10*, 743.
(41) Liu, K. J.; Ullmann, R. *Macromolecules* **1969**, *2*, 525.
(42) Allerhand, A.; Hailstone, R. K. *J. Chem. Phys.* **1972**, *56*,3718.